Antimicrobial Peptides

International Edition: DOI: 10.1002/anie.201706071
German Edition: DOI: 10.1002/ange.201706071

Bacteria-Assisted Activation of Antimicrobial Polypeptides by a Random-Coil to Helix Transition

Menghua Xiong, Zhiyuan Han, Ziyuan Song, Jin Yu, Hanze Ying, Lichen Yin, and Jianjun Cheng**

Abstract: *The application of antimicrobial peptides (AMPs) is largely hindered by their non-specific toxicity against mammalian cells, which is usually associated with helical structure, hydrophobicity, and charge density. A random coil-to-helix transition mechanism has now been introduced into the design of AMPs, minimizing the toxicity against mammalian cells while maintaining high antimicrobial activity. By incorporating anionic phosphorylated tyrosine into the cationic polypeptide, the helical structure of AMPs was distorted owing to the side-chain charge interaction. Together with the decreased charge density, the AMPs exhibited inhibited toxicity against mammalian cells. At the infectious site, the AMPs can be activated by bacterial phosphatase to restore the helical structure, thus contributing to strong membrane disruptive capability and potent antimicrobial activity. This bacteria-activated system is an effective strategy to enhance the therapeutic selectivity of AMPs.*

Treatment of drug-resistant bacteria remains a challenge in infectious disease, with limited and sometimes no drug choice.[1] Antimicrobial peptides (AMPs) have received much attention because their mechanism of function involves the targeting, perturbation, and damage of bacterial membrane, leading to bacteria death with limited resistance.[2] However, the application of AMPs is largely prohibited by their non-specific toxicity toward mammalian cells.[3] To obtain an ideal AMP with high selectivity toward bacterial cells, certain general structural parameters, such as size, charge, hydrophobicity, amphipathicity, solubility, and secondary structure of AMPs, have been studied.[2a,4] Often, the toxicity of AMPs is associated with their high charge density, high hydrophobicity, and secondary structures.[5] In particular, peptides with helical structure afford stronger membrane activity and toxicity than the corresponding non-helical peptides.[6] As such, the design of smart peptides with helix-coil transition provides a promising approach to enhance the selectivity of AMPs by controlling the secondary structure-dependent membrane activity as well as toxicity.[6a,7]

We recently developed a class of radially amphiphilic (RA) polypeptides with a long hydrophobic side chain and a terminal quaternary ammonium group on each amino acid residue.[8] These polypeptides adopt a stable α-helical conformation with a hydrophobic interior and a charged exterior shell around the helical surface, affording potent antimicrobial activity closely associated with their helical structure.[8] They offer several advantages over conventional AMPs, such as high stability against protease and simplicity of design. However, despite their strong antibacterial activity, the helical RA polypeptide PHLG-MMO bearing hydrophobic terminal amine groups (Figure 1) showed high toxicity to mammalian cells, as demonstrated by its 10% hemolytic concentration (HC10) at 24.7 μM and its minimal inhibitory concentration (MIC) against ATCC11778 and ATCC12608 bacterial strains at 3.1 and 6.2 μM, respectively.

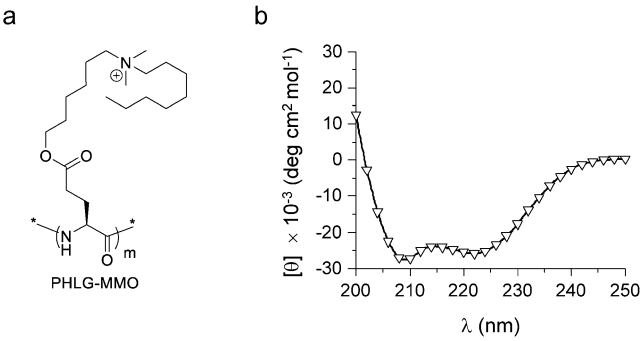

Figure 1. a) The chemical structure of helical antimicrobial polypeptide PHLG-MMO. b) Circular dichroism (CD) spectra of PHLG-MMO in aqueous solution at pH 7.

RA polypeptides have positively charged long hydrocarbon side chains. We envisioned that the insertion of phosphate groups onto the side chain of RA polypeptides would result in the distortion of helical conformation, which is due to intramolecular electrostatic interaction between the positively charged ammonium groups and the negatively charged phosphate groups (Scheme 1). The distortion of helical structure together with the decrease of overall cationic charge density would thus significantly reduce the toxicity of RA polypeptides (Scheme 1). As phosphatase is overly excreted in bacterial infectious sites,[9] if the inserted phosphate groups can be removed by bacterial phosphatase in the infectious sites, the phosphate-bearing RA polypeptides would resume the antibacterial activity specifically against

[*] Dr. M. Xiong, Z. Han, Dr. Z. Song, J. Yu, Dr. H. Ying, Prof. Dr. J. Cheng
Department of Materials Science and Engineering
University of Illinois at Urbana-Champaign
1304 W. Green Street, Urbana, IL 61801 (USA)
E-mail: jianjunc@illinois.edu
Prof. Dr. L. Yin, Prof. Dr. J. Cheng
Institute of Functional Nano & Soft Materials (FUNSOM), Jiangsu Key Laboratory for Carbon-Based Functional Materials & Devices
Soochow University, Suzhou 215123 (China)
E-mail: lcyin@suda.edu.cn

Supporting information for this article can be found under: https://doi.org/10.1002/anie.201706071.

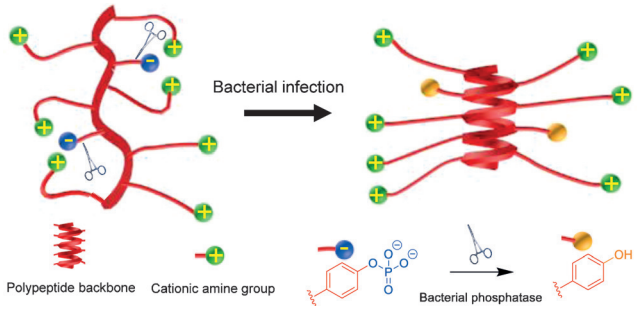

Scheme 1. Illustration of antimicrobial polypeptides with a random coil-to-helix conformation transition. Prior to reaching the bacterial infection site, the polypeptide adopts a random coiled conformation owing to the electrostatic interactions between positive and negative side chains, showing low toxicity. At the bacterial infection site, the polypeptide restores the helical structure upon phosphatase-mediated cleavage of the negatively charged phosphate groups, thereby affording strong membrane activity to kill bacteria. Green balls: cationic amine groups, blue balls: anionic phosphate groups, orange balls: neutral groups.

bacteria (Scheme 1). Herein, we report the design of phosphorylated polypeptides (Figure 2a) with a random coil-to-helix transition, showing remarkable antibacterial efficacy against ATCC11778, ATCC12608, and NRS384 bacterial strains with inhibited toxicity against mammalian cells.

RA random co-polypeptides poly(γ-6-(*N*,*N*-dimethyl-*N*-octylamino)hexyl-L-glutamate)-*r*-(poly-L-tyrosine)$_n$ (abbreviated as PHOT) were synthesized via ring-opening co-polymerization of γ-(6-chlorohexyl)-L-glutamate-*N*-carboxyanhydride (NCA) and L-tyrosine-NCA with 20 mol% and 10 mol% L-tyrosine-NCA (abbreviated as PHOT-1 and PHOT-2, respectively), followed by amination using *N*,*N*-dimethyloctylamine (Supporting Information, Figure S2a).[6d,10] The polypeptides adopted a helical structure according to circular dichroism (CD) spectra (Figure 2b), because the positively charged groups are separated from the backbone via a long, hydrophobic spacer.[6d] PHOPT were obtained by phosphorylation of the phenol residue of tyrosine of PHOT (Figure 2a). High-performance liquid chromatography (HPLC) analysis showed that the peak of PHOT-1 and PHOT-2 was clearly shifted from about 12 min to about 9 min after phosphorylation (Supporting Information, Figure S2c). ^{1}H-NMR spectra revealed that after phosphorylation, the protons from phenol ring were shifted to low field (Supporting Information, Figure S3), suggesting that majority of the phenol groups were successfully phosphorylated. The phosphorylated polypeptides (PHOPT-1 and PHOPT-2) showed distorted conformation (Figure 2b). As expected, the conformation-distorted PHOPT-1 and PHOPT-2 exhibited no hemolytic activity at a concentration up to 69 μM, while the helical PHOT polypeptides showed dramatically high hemolytic activity (Figure 2c). MTT assays on RAW 264.7 (macrophages), HEK293 (embryonic kidney cells), MCF 10A (breast epithelial cells), and IMR90 (fibroblast cells) also demonstrated that the non-helical PHOPT-2 exhibited much lower toxicity than the helical PHOT-2 (Supporting Information, Figure S4). We also synthesized racemic, non-helical polypeptides DL-PHOT-2 and DL-PHOPT-2 as negative controls (Supporting Information, Figure S5). DL-PHOT-2 showed high hemolytic activity while DL-PHOPT-2 showed no hemolytic activity even at a concentration of 67.2 μM (Supporting Information, Figure S5).

To evaluate whether the helix-distorted polypeptides can be activated by the bacterial phosphatase at the infectious sites to restore antibacterial activity, we measured the MIC of polypeptides against *Bacillus cereus* ATCC11778, *Staphylococcus aureus* ATCC12608, and methicillin-resistant *S. aureus* NRS384. As shown in Table 1, with the decrease of tyrosine content in the polypeptides from 20% (PHOT-1) to 10% (PHOT-2), higher antibacterial activity was noted. Non-helical phosphorylated PHOPT-1 and PHOPT-2 exhibited slightly reduced but still excellent antibacterial activity, as well as high selectivity as determined by the ratio of 10% hemolysis concentration to MIC. A selectivity value greater than 33 was observed with PHOPT-2 against ATCC12608 and NRS384 as opposed to red blood cells, showing great potential of this class of polypeptides in the treatment of bacterial infection. Furthermore, the phosphorylated, non-

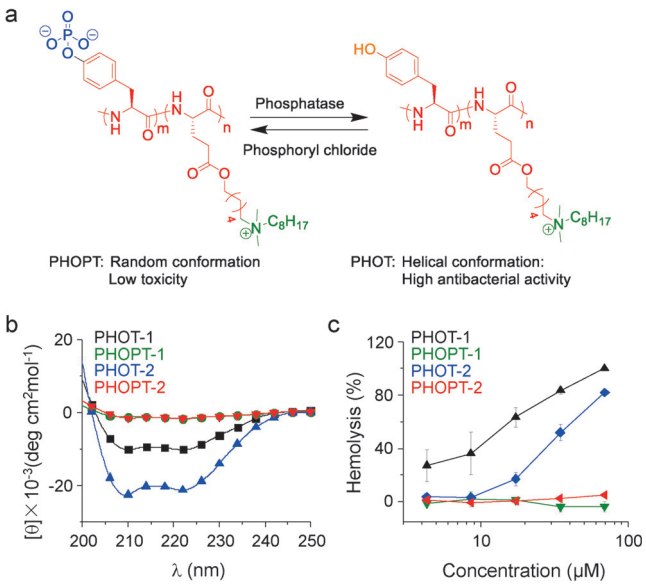

Figure 2. a) Illustration of PHOPT, which adopts a random coil conformation with low toxicity, and PHOT, which adopts a helical conformation with high antimicrobial activity. b) CD spectra of phosphorylated and non-phosphorylated polypeptides in aqueous solution. c) The hemolytic activity of phosphorylated and non-phosphorylated polypeptides at various concentrations.

Table 1: The antibacterial activity of bacteria activated polypeptides against bacterial strains (ATCC11778, ATCC12608, and NRS384).

Polypeptides	MIC [μM]		
	ATCC11778	ATCC12608	NRS384
PHOT-1	3.9	1.9	3.9
PHOPT-1	14.9	14.9	3.7
PHOT-2	0.5	0.5	0.5
PHOPT-2	4.1	2.1	2.1
DL-PHOT-2	2.1	8.4	1.1
DL-PHOPT-2	16.8	67.2	8.4

helical PHOPT-2 showed higher antibacterial activity than its racemic analogue DL-PHOPT-2. Considering that PHOPT-2 showed similar non-helical conformation and charge density as DL-PHOPT-2, the higher antibacterial activity of PHOPT-2 could be attributed to the restoration of helical conformation and accordingly the potent membrane activity upon cleavage of phosphate groups by the bacterial phosphatase. It should be noted that the non-helical DL-PHOT showed high antibacterial activity owing to its high charge density and hydrophobicity.

We next evaluated the batch-to-batch variation of polypeptide synthesis, aiming to evaluate whether the materials prepared from different batches would afford consistent antibacterial properties. As such, we synthesized another two batches of PHOT-2 and PHOPT-2, namely PHOT-2-2/2-3 and PHOPT-2-2/2-3, respectively. All three batches of polypeptides have similar molecular structures according to GPC, HPLC, CD, and NMR analyses (Supporting Information, Figures S3, S7), and showed similar hemolytic activity as well as antibacterial activity (Figure S8), which demonstrate excellent reproducibility in terms of the polypeptide synthesis and structure control.

We hypothesized that the potent antibacterial activity of PHOPT-2 was attributed to the restoration of helical structure and helix-dependent membrane activity after the cleavage of side phosphate groups by bacterial phosphatase. To demonstrate this, we first evaluated the degradation of a model compound Fmoc-Tyr(-PO3)-OH by HPLC after incubation with bacterial phosphatase (alkaline from *Escherichia coli*). Fmoc-Tyr(-PO3)-OH was converted into Fmoc-Tyr-OH upon 10 minute incubation with bacterial phosphatase at 37 °C (Supporting Information, Figure S9), indicating that the phosphorylated tyrosine can be easily dephosphorylated by bacterial phosphatase. We then incubated PHOPT-2 (8.2 μM) with bacterial phosphatase (0.06 UN mL^{-1}) under 37 °C, and monitored the degradation of PHOPT-2 by HPLC. The peak of PHOPT-2 at around 9 min was gradually reduced (Supporting Information, Figure S10), indicating the degradation of polypeptides by bacterial phosphatase. PHOPT-2 can also be degraded when incubated with bacterial culture medium (Supporting Information, Figure S11). However, when we incubated PHOPT-2 with the cell culture medium of Raw 264.7 cells for 24 h, no significant degradation of the polypeptide was noted (Supporting Information, Figure S12).

Because of the cleavage of phosphate on the polypeptide side chain terminals, PHOPT-2 restored its helical structure after treatment with phosphatase as evidenced by CD spectra (Figure 3a). We also examined the membrane-disruptive activity of PHOT-2, PHOPT-2, and phosphatase-treated PHOPT-2 on an anionic liposome that is widely used to simulate bacterial membranes.[11] After incubation of polypeptides with calcein-loaded liposomes, helical PHOT-2 induced notably higher calcein leakage level than the non-helical PHOPT-2 (Figure 3b), which correlated well with our previous findings that helical structure featured higher membrane-disruptive activity.[6d,8] After treatment with phosphatase, PHOPT-2 resulted in dramatically enhanced calcein leakage than its non-treated, non-helical analogue (PHOPT-2, Figure 3b), which substantiated that the restoration of the

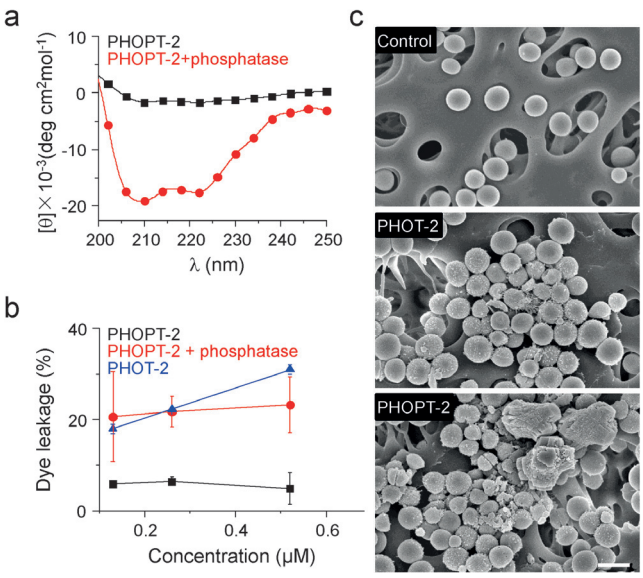

Figure 3. PHOPT-2 restores helix conformation by action of bacterial phosphatase. a) CD spectra of PHOPT-2 before and after treatment with phosphatase for 24 h. b) Calcein leakage levels from negatively charged liposomes after incubation with PHOT-2, PHOPT-2, and phosphatase-treated PHOPT-2 at various concentrations for 1 h. c) SEM images of ATCC12608 after treatment with PHOT-2 or PHOPT-2 at their MIC (0.5 and 2.1 μM, respectively). PBS was used as a control. The scale bar is 1 μm.

helical structure by bacterial phosphatase contributed to the recovery of membrane activity. In consistence with such restoration of membrane disruptive activity, PHOPT-2 could induce drastic damage to the bacterial membrane in a similar manner as the helical PHOT-2, as evidenced by morphological observation of ATCC12608 by scanning electron microscope (SEM, Figure 3c). Taken together, these findings collectively indicated that the phosphorylated, non-helical PHOPT-2 can be activated by bacterial phosphatase to restore helical structure and efficiently kill bacteria while affording low cytotoxicity to normal mammalian cells.

In conclusion, we introduced a random coil-to-helix transition mechanism into the design of AMPs. To the best of our knowledge, this is the first example of modulating the antimicrobial activity of polypeptide materials by controlling the transformation of secondary structures. Through such design, the AMPs exhibit high antimicrobial activity with inhibited toxicity against mammalian cells. It would be interesting to design sequence-controlled peptides by placing the phosphorylated tyrosine residue at different positions and to compare the difference of their biological activity, which will be among the explorations of our future work.

Acknowledgements

J.C. acknowledges support from the NSF (CHE-1153122) for the design and synthesis of polypeptide and the NIH (Director's New Innovator Award 1DP2OD007246 and 1R21EB013379) for the biological evaluation of the polypeptides. L.Y. acknowledges support from the National Natural

Science Foundation of China (51403145, 51573123), Ministry of Science and Technology of the People's Republic of China (2016YFA0201200), Collaborative Innovation Center of Suzhou Nano Science & Technology, and a Project Funded by the Priority Academic Program Development of Jiangsu Higher Education Institutions (PAPD). We thank Sigma–Aldrich for the supplement of NCA monomers.

Conflict of interest

The authors declare no conflict of interest.

Keywords: antimicrobial activity · bacteria · helical structures · peptides · phosphatase

How to cite: *Angew. Chem. Int. Ed.* **2017**, *56*, 10826–10829
Angew. Chem. **2017**, *129*, 10966–10969

[1] a) M. McKenna, *Nature* **2013**, *499*, 394–396; b) S. R. Modi, H. H. Lee, C. S. Spina, J. J. Collins, *Nature* **2013**, *499*, 219–222; c) G. Taubes, *Science* **2008**, *321*, 356–361; d) B. Mole, *Nature* **2013**, *499*, 398–400; e) K. M. G. O'Connell, J. T. Hodgkinson, H. F. Sore, M. Welch, G. P. C. Salmond, D. R. Spring, *Angew. Chem. Int. Ed.* **2013**, *52*, 10706–10733; *Angew. Chem.* **2013**, *125*, 10904–10932.

[2] a) C. D. Fjell, J. A. Hiss, R. E. W. Hancock, G. Schneider, *Nat. Rev. Drug Discovery* **2012**, *11*, 124–124; b) A. J. Krauson, O. M. Hall, T. Fuselier, C. G. Starr, W. B. Kauffman, W. C. Wimley, *J. Am. Chem. Soc.* **2015**, *137*, 16144–16152; c) M. Hughes, S. Debnath, C. W. Knapp, R. V. Ulijn, *Biomater. Sci.* **2013**, *1*, 1138–1142; d) L. Pu, J. B. Xu, Y. M. Sun, Z. Fang, M. B. Chan-Park, H. W. Duan, *Biomater. Sci.* **2016**, *4*, 871–879; e) G. T. Qin, A. Lopez, C. Santos, A. M. McDermott, C. Z. Cai, *Biomater. Sci.* **2015**, *3*, 771–778.

[3] a) Z. Y. Ong, N. Wiradharma, Y. Y. Yang, *Adv. Drug Delivery Rev.* **2014**, *78*, 28–45; b) V. W. L. Ng, X. Y. Ke, A. L. Z. Lee, J. L. Hedrick, Y. Y. Yang, *Adv. Mater.* **2013**, *25*, 6730–6736; c) M. F. Ilker, K. Nusslein, G. N. Tew, E. B. Coughlin, *J. Am. Chem. Soc.* **2004**, *126*, 15870–15875; d) B. P. Mowery, S. E. Lee, D. A. Kissounko, R. F. Epand, R. M. Epand, B. Weisblum, S. S. Stahl, S. H. Gellman, *J. Am. Chem. Soc.* **2007**, *129*, 15474–15475; e) I. S. Radzishevsky, S. Rotem, D. Bourdetsky, S. Navon-Venezia, Y. Carmeli, A. Mor, *Nat. Biotechnol.* **2007**, *25*, 657–659; f) F. Nederberg, Y. Zhang, J. P. K. Tan, K. J. Xu, H. Y. Wang, C. Yang, S. J. Gao, X. D. Guo, K. Fukushima, L. J. Li, J. L. Hedrick, Y. Y. Yang, *Nat. Chem.* **2011**, *3*, 409–414.

[4] a) W. Aoki, M. Ueda, *Pharmaceuticals* **2013**, *6*, 1055–1081; b) Y. B. Huang, J. F. Huang, Y. X. Chen, *Protein Cell* **2010**, *1*, 143–152; c) A. A. Bahar, D. Ren, *Pharmaceuticals* **2013**, *6*, 1543–1575; d) E. Glukhov, M. Stark, L. L. Burrows, C. M. Deber, *J. Biol. Chem.* **2005**, *280*, 33960–33967; e) A. C. Engler, N. Wiradharma, Z. Y. Ong, D. J. Coady, J. L. Hedrick, Y. Y. Yang, *Nano Today* **2012**, *7*, 201–222.

[5] a) M. A. Sani, F. Separovic, *Acc. Chem. Res.* **2016**, *49*, 1130–1138; b) D. O. Ulaeto, C. J. Morris, M. A. Fox, M. Gumbleton, K. Beck, *Antimicrob. Agents Chemother.* **2016**, *60*, 1984–1991; c) Y. Shai, *Biochim. Biophys. Acta Biomembr.* **1999**, *1462*, 55–70; d) G. N. Tew, D. H. Liu, B. Chen, R. J. Doerksen, J. Kaplan, P. J. Carroll, M. L. Klein, W. F. DeGrado, *Proc. Natl. Acad. Sci. USA* **2002**, *99*, 5110–5114.

[6] a) L. Yin, H. Tang, K. H. Kim, N. Zheng, Z. Song, N. P. Gabrielson, H. Lu, J. Cheng, *Angew. Chem. Int. Ed.* **2013**, *52*, 9182–9186; *Angew. Chem.* **2013**, *125*, 9352–9356; b) N. P. Gabrielson, H. Lu, L. C. Yin, D. Li, F. Wang, J. J. Cheng, *Angew. Chem. Int. Ed.* **2012**, *51*, 1143–1147; *Angew. Chem.* **2012**, *124*, 1169–1173; c) H. Y. Tang, L. C. Yin, K. H. Kim, J. J. Cheng, *Chem. Sci.* **2013**, *4*, 3839–3844; d) H. Lu, J. Wang, Y. G. Bai, J. W. Lang, S. Y. Liu, Y. Lin, J. J. Cheng, *Nat. Commun.* **2011**, *2*, 206.

[7] a) J. R. Kramer, T. J. Deming, *J. Am. Chem. Soc.* **2014**, *136*, 5547–5550; b) J. R. Kramer, T. J. Deming, *J. Am. Chem. Soc.* **2012**, *134*, 4112–4115; c) H. M. Wang, Z. Q. Q. Feng, Y. Z. Wang, R. Zhou, Z. M. Yang, B. Xu, *J. Am. Chem. Soc.* **2016**, *138*, 16046–16055; d) J. Zhou, X. W. Du, N. Yamagata, B. Xu, *J. Am. Chem. Soc.* **2016**, *138*, 3813–3823.

[8] M. Xiong, M. W. Lee, R. A. Mansbach, Z. Song, Y. Bao, R. M. Peek, Jr., C. Yao, L. F. Chen, A. L. Ferguson, G. C. Wong, J. Cheng, *Proc. Natl. Acad. Sci. USA* **2015**, *112*, 13155–13160.

[9] a) R. H. Glew, E. C. Heath, *J. Biol. Chem.* **1971**, *246*, 1566–1574; b) A. J. Standish, R. Morona, *Antioxid. Redox Signaling* **2014**, *20*, 2274–2289; c) M. H. Xiong, Y. J. Li, Y. Bao, X. Z. Yang, B. Hu, J. Wang, *Adv. Mater.* **2012**, *24*, 6175–6180.

[10] a) L. C. Yin, Z. Y. Song, Q. H. Qu, K. H. Kim, N. Zheng, C. Yao, I. Chaudhury, H. Y. Tang, N. P. Gabrielson, F. M. Uckun, J. J. Cheng, *Angew. Chem. Int. Ed.* **2013**, *52*, 5757–5761; *Angew. Chem.* **2013**, *125*, 5869–5873; b) H. Lu, J. J. Cheng, *J. Am. Chem. Soc.* **2007**, *129*, 14114–14115.

[11] Z. Oren, Y. Shai, *Biochemistry* **1997**, *36*, 1826–1835.

Manuscript received: June 14, 2017
Accepted manuscript online: June 28, 2017
Version of record online: July 28, 2017

